Title

A novel loss-of-function mutation in Npr2 clarifies primary role in female reproduction and reveals a potential therapy for acromesomelic dysplasia, Maroteaux type

Journal

Human Molecular Genetics, 22(2)

ISSN

0964-6906

Authors

Geister, Krista A
Brinkmeier, Michelle L
Hsieh, Minnie
et al.

Publication Date

2013-01-15

DOI

10.1093/hmg/dds432

Peer reviewed

Human Molecular Genetics, 2013, Vol. 22, No. 2 **345–357**
doi:10.1093/hmg/dds432
Advance Access published on October 12, 2012

A novel loss-of-function mutation in *Npr2* clarifies primary role in female reproduction and reveals a potential therapy for acromesomelic dysplasia, Maroteaux type

Krista A. Geister[1], Michelle L. Brinkmeier[2], Minnie Hsieh[4,†], Susan M. Faust[1,‡], I. Jill Karolyi[2], Joseph E. Perosky[3], Kenneth M. Kozloff[3], Marco Conti[4] and Sally A. Camper[1,2,*]

[1]Graduate Program in Cellular and Molecular Biology, [2]Department of Human Genetics, and [3]Orthopedic Surgery and Biomedical Engineering, University of Michigan, Ann Arbor, MI 48109, USA, and [4]Department of Obstetrics and Gynecology and Reproductive Sciences, University of California San Francisco, San Francisco, CA 94143, USA

Received August 1, 2012; Revised and Accepted October 8, 2012

We discovered a new spontaneous mutant allele of *Npr2* named *peewee* (*pwe*) that exhibits severe disproportionate dwarfism and female infertility. The *pwe* phenotype is caused by a four base-pair deletion in exon 3 that generates a premature stop codon at codon 313 (L313X). The *Npr2*$^{pwe/pwe}$ mouse is a model for the human skeletal dysplasia acromesomelic dysplasia, Maroteaux type (AMDM). We conducted a thorough analysis of the female reproductive tract and report that the primary cause of *Npr2*$^{pwe/pwe}$ female infertility is premature oocyte meiotic resumption, while the pituitary and uterus appear to be normal. *Npr2* is expressed in chondrocytes and osteoblasts. We determined that the loss of *Npr2* causes a reduction in the hypertrophic and proliferative zones of the growth plate, but mineralization of skeletal elements is normal. Mutant tibiae have increased levels of the activated form of ERK1/2, consistent with the idea that natriuretic peptide receptor type 2 (NPR2) signaling inhibits the activation of the MEK/ERK mitogen activated protein kinase pathway. Treatment of fetal tibiae explants with mitogen activated protein kinase 1 and 2 inhibitors U0126 and PD325901 rescues the *Npr2*$^{pwe/pwe}$ growth defect, providing a promising foundation for skeletal dysplasia therapeutics.

INTRODUCTION

Disruptions in skeletal development and growth are classified as skeletal dysplasias and are an important contributor to severe short stature, occurring in approximately 1 out of every 5000 births (1). The effects on individuals with skeletal dysplasia can range from relatively minor to lethality (1–3) and multiple organ systems can be affected (1). The advent and improved accessibility to high-throughput sequencing technologies has brought forth a wealth of information regarding the genetic causes of skeletal dysplasias (1,4). According to the most recent nosology, there are 456 forms of skeletal dysplasia, of which 316 have been associated with mutations in one or more of 226 genes (4). This means that approximately 70% of the skeletal dysplasias have known genetic causes (4). The genetic causes of the remaining forms are currently unknown (1,3,4), and even those forms that have a known genetic cause may not have a clear molecular mechanism (1). Animal models of skeletal dysplasia have been useful in understanding the mechanisms by which these genes regulate proper skeletal development and growth and contribute to the pathology of skeletal dysplasia (1,5–7).

Some disorders of the skeleton also affect the reproductive organs (8–11). Infertility is estimated to affect 15% of the global population and 25% of these cases are idiopathic (12). There has been a surge of interest in the mechanisms of female infertility and sub-fertility with respect to reproductive aging, as many women in developed countries are delaying

*To whom correspondence should be addressed at: Sally A. Camper, 4909 Buhl Bldg., 1241 Catherine St., Department of Human Genetics, University of Michigan, Ann Arbor, MI 48109-5618, USA. Tel: +1 734 763 0682; Fax: +1 734 763 3784; Email: scamper@umich.edu
†Present address: Health Interactions, San Francisco, CA 94111, USA.
‡Present address: Gene Therapy Program, University of Pennsylvania, Philadelphia, PA 19104, USA.

their age of first conception past their early 20s, when female fertility is at its zenith (13). Mouse models of female infertility have offered much in the way of understanding the genetic regulation of female fertility (14,15).

We have discovered a novel recessive, mutant allele of *Npr2*, the gene that encodes natriuretic peptide receptor type 2 (NPR2), which we have named *peewee* (*pwe*). The mutant mice have growth insufficiency, skeletal dysplasia and female infertility. Mutations in *NPR2* cause a rare form of recessive skeletal dysplasia in humans, acromesomelic dysplasia, Maroteaux type (AMDM) (16), which affects the middle and distal portions of limbs and the shape of vertebrae (16,17). *Npr2* encodes a membrane-bound guanylyl cyclase that generates the secondary messenger cyclic guanosine monophosphate (cGMP) upon binding its ligand, C-type natriuretic peptide (CNP) (18).

We report a comprehensive analysis of the role of *Npr2* in the regulation of female fertility, and evidence that pharmacological inhibition of mitogen activated protein kinase 1 and 2 (MEK1/2) is sufficient to rescue the *peewee* growth defect in tibial explants. These findings offer promising clues as to signaling pathways that could be therapeutic targets in the treatment of AMDM and other forms of skeletal dysplasia.

RESULTS

The *peewee* growth defect

The *peewee* (*pwe*) mouse arose on the NAW/WI background, was outcrossed to obtain hybrid vigor and was maintained as a stock by breeding heterozygotes. Only 12% of the progeny were mutant, which is lower than expected for autosomal recessive inheritance. Outcrossing to *Mus castaneus* supported homozygote viability. Mutants constituted 27% of the progeny of this F1 × F1 intercross (28/103), consistent with the expected Mendelian ratio for an autosomal recessive allele.

Pwe homozygous mutants exhibit growth delay and disproportionate dwarfism that is evident at 2 weeks of age (Fig. 1). Body weight and crown-rump length of mutants are 54 and 77%, respectively, of their unaffected littermates (Table 1). *pwe* mice have a characteristic cranial dysmorphology that includes a domed skull and short snout (Fig. 1A). Malocclusion is frequent, but incompletely penetrant. All bones formed through endochondral ossification are significantly reduced in length (Table 1 and Fig. 2A, A–L).

The proximal skeletal elements of the appendicular skeleton (femur and humerus) are the most severely affected in the *pwe* mouse (Table 1 and Fig. 2A, C and E). All skeletal elements formed through endochondral ossification are $\leq$75% the length of unaffected skeletal elements (Table 1 and Fig. 2A, A–L). There is no reduction in the width of the skull, femur (thinner dimension) or ribs (Table 1). A fully penetrant aspect of the phenotype is a notch on the dorsal surface of the atlas (Fig. 2A and K).

Sections through 5-week-old male tibial growth plates suggest that the skeletal growth defect in *pwe* mice stems from a disruption in the regulation of chondrocyte differentiation, and potentially proliferation, due to the reduction in the height of the hypertrophic and proliferative zones of the growth plate (Fig. 2B). However, all zones of the growth plate are present, and their organization is maintained, meaning that the disturbance in skeletal growth may be due to a disruption in the number or rate in which the chondrocytes progress through the zones of the growth plate (Fig. 2B).

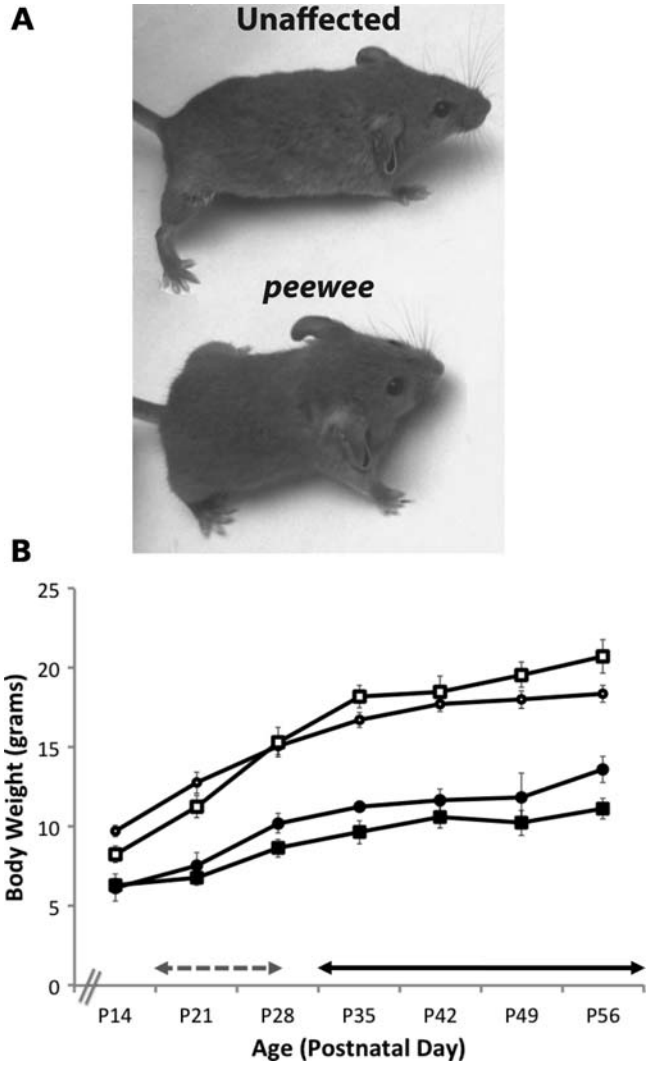

Figure 1. Decreased body size and growth delay in *peewee* mice. (**A**) Comparison of an unaffected littermate and a *peewee* mutant reveals a decreased body size and cranial dysmorphology by 2 weeks of age (P14). (**B**) Growth curve (unaffected males: open squares, unaffected females: open circles; affected males: closed squares; affected females: closed circles) showing a significant decrease in body weight in mutants by P14. Arrows below indicate the range of ages at vaginal opening in unaffected (dashed arrow, $n = 11$) and affected (solid arrow, $n = 6$) females.

Molecular identification of the *peewee* mutation

Analysis of DNA samples from 15 affected animals from a [(*pwe*/+) × CAST/Ei$^{+/+}$] F1 × F1 intercross with a single nucleotide polymorphism (SNP)-mapping panel (19) placed the locus in a region on proximal mouse chromosome 4. Analysis of additional animals with more markers confirmed this location and narrowed the interval. The genotype of affected mice placed the mutation distal to the microsatellite marker

Table 1. Disproportionate dwarfism in *peewee* mutants

	Unaffected	*peewee*	Ratio[a]	*P*-value
Body weight (g)	25 ± 1	16 ± 1	0.54	0.001
Length of body and skeletal elements (mm)[b]				
Crown to rump	71.05 ± 0.96	54.43 ± 0.94	0.77	0.0003
Radius	10.40 ± 0.19	5.28 ± 0.13	0.51	<0.0001
Ulna	12.83 ± 0.25	7.16 ± 0.18	0.56	<0.0001
Femur	15.12 ± 0.19	8.49 ± 0.21	0.56	<0.0001
Humerus	11.52 ± 0.17	7.36 ± 0.17	0.64	<0.0001
Tibia	15.84 ± 1.01	10.28 ± 0.29	0.65	0.001
Illium	17.09 ± 0.39	12.59 ± 0.13	0.74	<0.0001
Scapula	10.93 ± 0.15	8.22 ± 0.15	0.75	<0.0001
Skull	23.38 ± 0.31	19.89 ± 0.41	0.85	0.0003
Width of skeletal elements (mm)[b]				
L6 vertebrae	3.51 ± 0.09	2.48 ± 0.08	0.71	0.001
Femur[c] (a)	2.08 ± 0.04	1.83 ± 0.03	0.88	0.0005
Femur[c] (b)	1.47 ± 0.04	1.36 ± 0.04	0.93	NS
Skull	11.52 ± 0.22	11.28 ± 0.35	0.98	NS
Rib	0.78 ± 0.05	0.83 ± 0.03	1.06	NS

[a]Ratio of *peewee* to unaffected.
[b]Individual skeletal elements are listed from most affected to least affected.
[c]Femurs were measured in the thicker (a) and thinner (b) dimensions.

D4Mit93 (Fig. 3A), and analysis of unaffected animals narrowed the critical interval to a 3 Mb region between *D4Mit212* and *D4Mit109* (Fig. 3A, one animal per marker), which contains more than 80 genes and corresponds to human chromosome 9p13.3. A search for skeletal dysplasias associated with this region of human chromosome 9 identified AMDM, which is caused by loss-of-function mutations of *Npr2* in humans (16,17). Sequencing of *Npr2* in known *pwe* mutants revealed a four base-pair deletion in exon 3 of *Npr2* (Fig. 3B). This deletion results in a frameshift that generates a premature stop codon at codon 313, which encodes a leucine residue in the wild-type and reference open reading frame (L313X, Fig. 3B). Genotyping this mutation revealed that one apparently affected animal was actually a runted heterozygote, explaining the erroneous exclusion of *Npr2* as a potential candidate gene early in our analysis (Fig. 3A, asterisk).

Npr2 encodes a membrane-bound guanylyl cyclase that is present at the plasma membrane as a dimer (18). Mutations in human AMDM patients occur throughout the length of the encoded NPR2 protein (16,20) (Fig. 3C). The premature stop codon at codon 313 in *Npr2*$^{pwe/pwe}$ mice truncates NPR2 within the ligand-binding domain (18) (Fig. 3C). Without an intact ligand-binding domain or any of the domains C-terminal to the premature stop codon, any translated protein from the *pwe* allele is predicted to be nonfunctional, generating a null allele (Fig. 3C). The growth insufficiency of *pwe* mutants is indistinguishable from that reported for other mouse null alleles of *Npr2* (21–24).

Npr2$^{pwe/pwe}$ female infertility

We tested fertility by mating wild-type mice with *Npr2*$^{pwe/pwe}$ mutants. Males were sub-fertile, but had no obvious abnormalities in the penian bone or testis histology (data not shown). Over a 3-month period, all unaffected females ($n = 3$) bore litters, while none of the *Npr2*$^{pwe/pwe}$ females ($n = 3$) bore litters (data not shown). *Npr2* is expressed at all levels of the female reproductive tract in the rodent (18,25–28). Thus, *Npr2*$^{pwe/pwe}$ female infertility could be due to defects in any or all of these organs. We undertook a systematic approach to uncover critical sites of *Npr2* action in the female reproductive tract.

We tested whether *Npr2*$^{pwe/pwe}$ females experienced puberty normally by observing the date of vaginal opening as an indicator of the onset of puberty in mice (29–31). The control animals experienced vaginal opening on average at postnatal day 21 (P21) as expected (Fig. 1B, range P18–P28, $n = 11$), while *Npr2*$^{pwe/pwe}$ females experienced vaginal opening from P33–P84 (Fig. 1B, $n = 6$). The extensive delay in puberty in individual *Npr2*$^{pwe/pwe}$ females appears to correlate with their body weight (Supplementary Material, Fig. S1A). Body weight is a known predictor of the onset of puberty in mice (30,31) and humans (32).

To determine whether post-pubertal *Npr2*$^{pwe/pwe}$ females were capable of cycling through estrus, vaginal smears were taken for 20 consecutive days and estrous stage was assigned by vaginal cytology (29). Control ($n = 7$) and *Npr2*$^{pwe/pwe}$ ($n = 4$) females cycled normally through all stages of the estrous cycle during this 20-day period (Fig. 4A). The amount of time spent in each of the stage of the cycle did not differ between mutants and controls (Fig. 4A). Thus, while *Npr2*$^{pwe/pwe}$ females have a delay in the onset of puberty, they are capable of cycling through estrus normally, suggesting that the hypothalamus and pituitary are functioning properly to regulate the estrous cycle (29,33). The diestrus uterine histology of *Npr2*$^{pwe/pwe}$ females is normal at 12 weeks of age, indicating that the uterine tissues, including the endometrium, myometrium and stromal glands, are intact (Fig. 4C).

To assess ovarian follicle development in the *Npr2*$^{pwe/pwe}$ female, we stimulated prepubertal females with pregnant mare's serum gonadotropin (PMSG), which stimulates follicle growth to the preovulatory stage. Oocytes are arrested around birth at prophase I, and this is morphologically distinguished by the presence of a germinal vesicle (13,15,34–36). The germinal vesicle is normally maintained until the preovulatory follicle receives the surge of luteinizing hormone (LH) that promotes meiotic resumption and ovulation (13,15,34–36). At this point, the germinal vesicle will break down, the meiotic spindle is formed and the first meiotic division is completed with the extrusion of the first polar body (13,15,34–36). Preovulatory follicles in the ovaries of PMSG-primed control females contained oocytes (either released from ovarian follicles or in sections of whole ovaries) with intact germinal vesicles (Fig. 5A). However, *Npr2*$^{pwe/pwe}$ oocytes had progressed prematurely through meiosis; virtually all oocytes examined underwent premature germinal vesicle breakdown (GVBD) (Fig. 5A). Some had formed meiotic spindles, or extruded one or even two polar bodies (Fig. 5A). cGMP, which is generated by NPR2, is known to inhibit progression through meiosis (37,38). The level of cGMP in *Npr2*$^{pwe/pwe}$ antral follicles was reduced to undetectable levels (Fig. 5A). Thus, *Npr2* is essential for cGMP production and maintenance of meiotic arrest in the oocyte.

To determine whether *Npr2*$^{pwe/pwe}$ females were capable of releasing fertilizable oocytes into the oviducts, we superovulated prepubertal *Npr2*$^{pwe/pwe}$ females as described in the Methods section and mated them with a proven wild-type

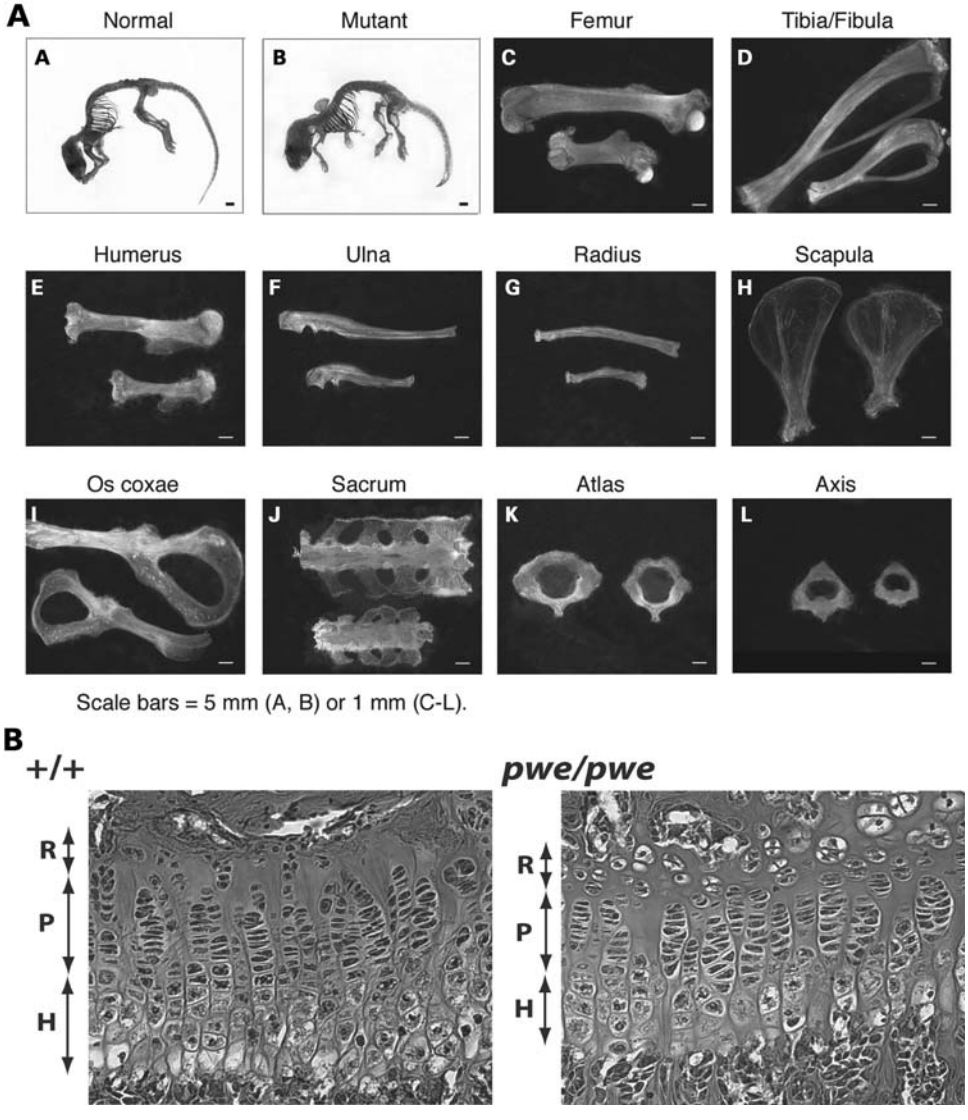

Figure 2. Skeletal phenotype of *peewee* mice. (A) Whole skeletal preparations individual skeletal elements from mutants and normal littermates. Unaffected (**A**) and affected whole skeletons (**B**) are shown. Individual skeletal elements from unaffected and affected animals were dissected from whole skeletons (**C**–**L**). K: C2, or the atlas: mutant C2 vertebrae have an abnormal notch on the dorsal side. (B) Bone histology. Sections through 5-week-old male proximal tibiae at the level of the growth plate (×40 magnification). Arrows indicate hypertrophic (H), proliferative (P) and resting zones (R).

male. *Npr2*$^{pwe/pwe}$ females ovulated fewer oocytes than controls (Fig. 5B), and they underwent oocyte fragmentation, a precursor to oocyte cell death (39). None of the *Npr2*$^{pwe/pwe}$ oocytes progressed to the two-cell embryo stage.

We tested the natural ability of *Npr2*$^{pwe/pwe}$ females to ovulate by conducting natural mating experiments with mature, post-pubertal animals. *Npr2*$^{pwe/pwe}$ females released similar numbers of oocytes when compared with controls [(*Npr2*$^{pwe/pwe}$, $n = 6$ and control, $n = 6$), data not shown). We measured the levels of follicle-stimulating hormone (FSH) and estradiol. Levels of both the hormones at diestrus were normal (Table 2). Levels of LH and FSH from individual male and female pituitaries determined by radioimmunoassay were also normal (data not shown). Sections through *Npr2*$^{pwe/pwe}$ ovaries at 8 and 12 weeks revealed the presence of corpora lutea (Fig. 4B), consistent with ovulation (33,40). Together, these data indicate that the hypothalamus and pituitary of *Npr2*$^{pwe/pwe}$ females are functioning well enough to support ovulation and the ovary responds with appropriate steroid hormone production (33,40).

Npr2 and bone tissue mineral density

Npr2 is expressed in osteoblasts as well as chondrocytes (41), and data suggest that CNP-NPR2 signaling may augment osteoblast differentiation in combination with other factors (42). It is hypothesized that many disruptions in the growth plate also affect the normal function of osteoblasts or osteoclasts (7). We assessed whether bone was defective in mineralization or integrity by microscopic-computed tomography (microCT) scans of 12-week-old male femurs and L4 vertebrae (control, $n = 6$; mutant, $n = 7$). No major deficits in the

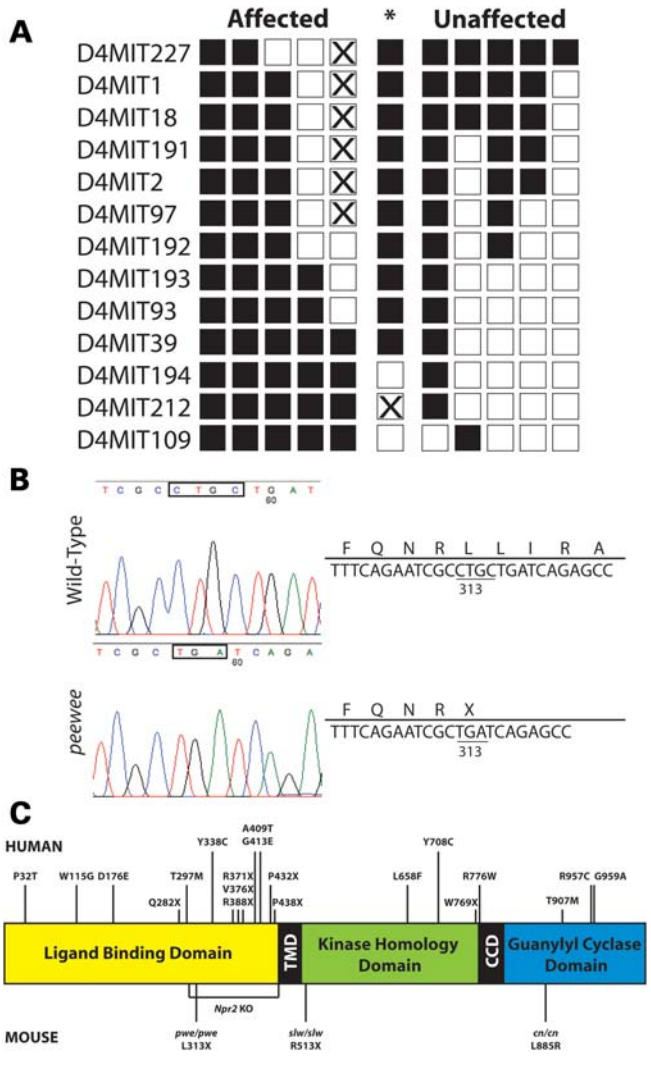

Figure 3. The *peewee* phenotype is caused by a mutation in *Npr2*. (**A**) Mapping of the *peewee* critical interval in progeny of an F1 × F1 cross with *Mus castaneus.* Haplotypes are shown for selected mice, and genotypes indicating homozygous or heterozygous *Mus castaneus* alleles are open boxes, homozygous *peewee* stock are black boxes and boxes marked with an 'X' indicate that data are unavailable. The critical interval is limited to the region between *D4MIT212* and *D4MIT109*. A single animal that appeared affected genotypes as a heterozygote in the critical interval (*). (**B**) DNA sequencing of genomic DNA reveals that *peewee* animals have a 4 bp deletion in exon 3 of *Npr2*. This generates a premature stop codon at codon 313 (L313X). (**C**) Missense and nonsense mutations (true nonsense and those formed from frame shift mutations) in NPR2 are found in AMDM patients (16,20,53,54), spontaneous mutant *Npr2*$^{slw/slw}$ and *Npr2*$^{cn/cn}$ mice (22–24), and a targeted KO animal (21). (TMD, transmembrane domain; CCD, coiled-coil domain).

mineralization of trabecular and cortical bones of *Npr2*$^{pwe/pwe}$ males were observed (Supplementary Material, Fig. S1B). Therefore, while *Npr2* is expressed in osteoblasts, the loss of *Npr2* in this cell type does not appear to affect proper mineralization of long bones and vertebral elements.

Elevated levels of phosphorylated ERK1/2 in *Npr2*$^{pwe/pwe}$ tibiae

The fibroblast growth factor (FGF) signaling axis is a potent activator of the MEK/ERK mitogen activated protein kinase (MAPK) pathway in the growth plate (43,44) (Fig. 6A). Gain-of-function mutations in the gene that encodes FGF receptor 3 (FGFR3) cause achondroplasia in humans (1,6,7,44,45). In cultured chondrocytes, activation of MEK/ERK leads to a reduction in the production of extracellular matrix proteins, differentiation and possibly proliferation (43,44). The cGMP generated by NPR2 upon binding CNP activates cGMP-dependent protein kinase II (PKGII), which goes on to inhibit the activation of RAF-1, the activator of MEK1/2 (43). Thus, NPR2 signaling halts the MEK/ERK MAPK cascade at the level of RAF-1 (Fig. 6A) through its activation of PKGII (43) *in vitro*.

We hypothesized that if *Npr2*$^{pwe/pwe}$ mice lack the critical receptor required for MEK/ERK inhibition, they should have increased levels of phosphorylated ERK1/2. Western blot analysis was performed using postnatal day three (P3) tibial lysates. Higher levels of phosphorylated ERK1/2 were observed in lysates prepared from mutant tibiae relative to wild-type (Fig. 6B). Thus, signaling through NPR2 inhibits the activation of the MEK/ERK MAPK pathway in intact bone.

Therapy for the *Npr2*$^{pwe/pwe}$ growth defect

We reasoned that treatment of *Npr2*$^{pwe/pwe}$ mice with a pharmacological inhibitor of the MEK/ERK MAPK pathway might improve bone growth. We cultured fetal tibiae harvested at embryonic day 16.5 for six days as explants in the presence of vehicle (DMSO) or the MEK1/2 inhibitors U0126 and PD325901 (Fig. 7A) (21,46–50). PD325901 is a potent MEK1/2 inhibitor (50), and has been used to study mouse cancers (46,47). After the culture period, the tibiae were photographed and measured (Fig. 7). Mutant tibiae were shorter than wild-type after treatment with vehicle, and both inhibitors induced growth of wild-type and mutant tibiae. PD235901 induced more growth than U0126. Two-way ANOVA and Bonferroni post-hoc analysis confirmed that the effects of both treatments were highly significant (Fig. 7B, $P < 0.0001$, $n = 16$ of both genotypes for U0126, $n = 7$ of both genotypes for PD325901). Drug-induced growth of the normal tibiae suggests that CNP signaling is rate limiting in normal mice. Western blots revealed reduced phosphorylated ERK1/2 in U0126-treated animals, demonstrating that the drug effectively inhibited MEK/ERK activation in explants from normal and mutant mice (Fig. 7C).

The histology of sections from cultured tibiae suggested that the primary effect of U0126 on wild-type and mutant tibiae was to expand the size of the hypertrophic zone (Fig. 7A). *In situ* hybridization was performed to assess expression of *Col10a1* (51) (collagen 10, alpha subunit), a marker of hypertrophic chondrocytes (Fig. 7A). The cells in this expanded zone of the growth plate are marked with *Col10a1* transcripts, confirming that these are hypertrophic chondrocytes.

DISCUSSION

We have identified the genetic defect in *peewee*, a new spontaneous mutant allele of *Npr2*, with growth insufficiency and female infertility. The phenotype is caused by a 4-bp deletion in exon 3 of *Npr2* that generates a premature stop codon at

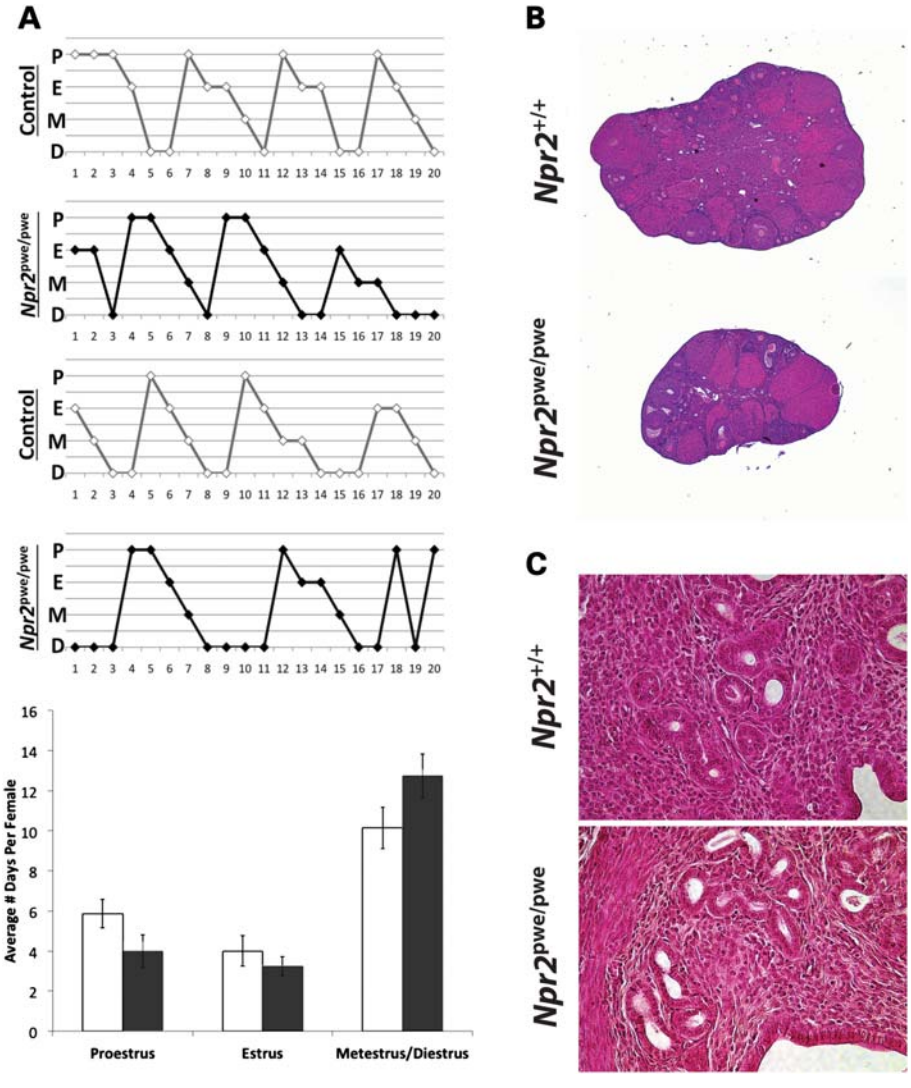

Figure 4. *Npr2*$^{pwe/pwe}$ females cycle through estrus have normal levels of estradiol and FSH, form corpora lutea and have normal uterine histology. (**A**) Estrous cycles of two representative *Npr2*$^{pwe/pwe}$ females (black symbols and lines) and controls (white symbols and grey lines) over a 20-day consecutive period show all stages of the estrous cycle (P = proestrus, E = estrus, M = metestrus, and D = diestrus, top panel). *Npr2*$^{pwe/pwe}$ females spend similar amounts of time in each stage of the estrous cycle as controls. (**B**) Eight-week *Npr2*$^{pwe/pwe}$ ovaries contain corpora lutea at metestrus. (**C**) Twelve-week *Npr2*$^{pwe/pwe}$ uterine histology at diestrus is normal, including the presence of stromal glands.

codon 313. This leads to truncation of the receptor within the ligand-binding domain and a predicted null allele due to the loss of all domains C-terminal to the mutation. Other null alleles of *Npr2* with similar skeletal and growth insufficiencies have been reported, but previous characterization focused on other aspects of *Npr2* function including blood pressure regulation and gastrointestinal tract function (21,24). Here we report a comprehensive analysis of female infertility and a bone growth in response to pharmacotherapy.

Since *Npr2* is expressed in all the major organs of the female reproductive tract (18,25–28), we addressed the possibility that multiple organs could contribute to *peewee* female infertility. We show for the first time that *Npr2*-deficient females exhibit a delay in puberty, and this delay correlates with the body size (30,31). Once *Npr2*$^{pwe/pwe}$ females reach puberty, they progress through all stages of the estrous cycle and are capable of ovulating in response to exogenous and natural stimulation. Our results differ from previous reports that the *Npr2* knock-out (KO) allele caused loss of cycling, uterine atrophy, reduced endometrial and myometrial layers, and absent stromal glands (21). The differences are likely due to genetic background effects. We characterized *Npr2*$^{pwe/pwe}$ on a mixed background that supports viability, but the mutation has reduced viability on other backgrounds, similar to reports for other *Npr2* alleles. Susceptible background strains may offer less compensation for *Npr2* deficiency in a variety of organs that express *Npr2*, including the uterus and pituitary gland. Genetic compensation could involve variable cross talk between other natriuretic peptide receptors and ligands.

Npr2$^{pwe/pwe}$ females have normal serum levels of FSH and estradiol at diestrus and naturally ovulate, indicating that

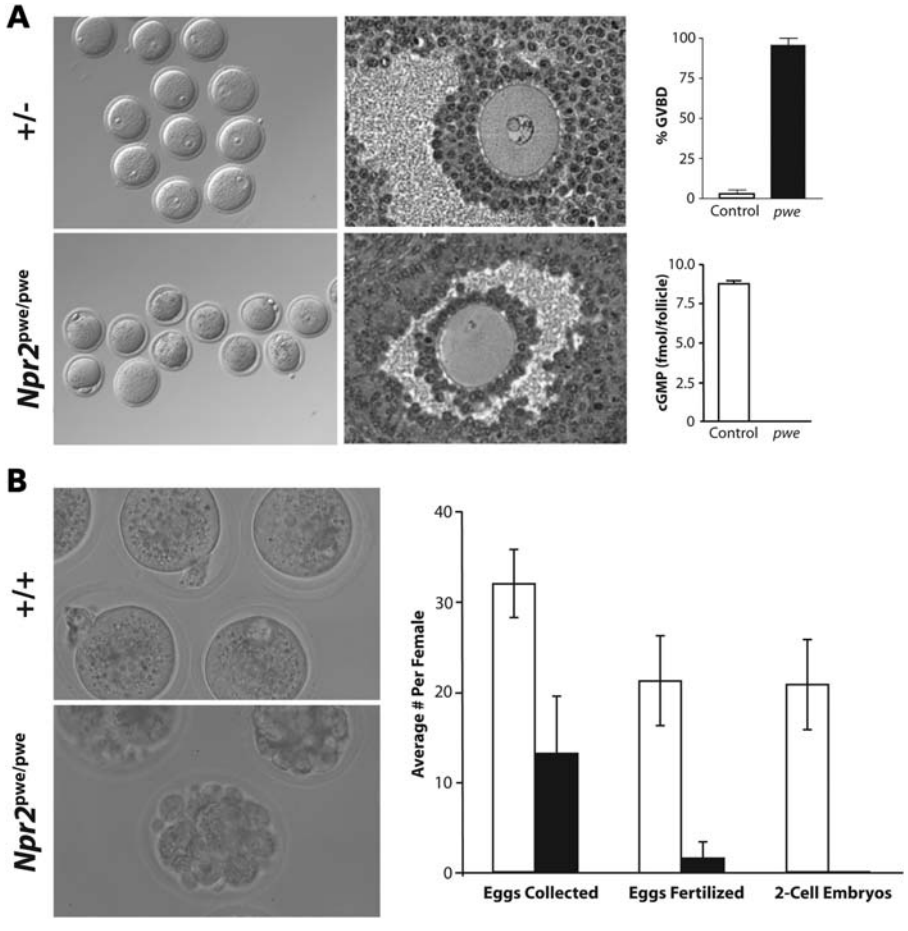

Figure 5. *Npr2*$^{pwe/pwe}$ female infertility is caused by a failure in meiotic arrest, leading to the release of oocytes that are not viable. (**A**) Oocytes from unaffected (+/−) and *Npr2*$^{pwe/pwe}$ mice were released from prepubertal PMSG-primed antral follicles by needle puncture and examined by light microscopy with DIC optics (left). Almost all oocytes had a single pronucleus while most oocytes from *Npr2*$^{pwe/pwe}$ follicles exhibited GVBD and premature formation of polar bodies. The percentage of oocytes that underwent GVBD is shown at the far right (top). Data are the mean ± SEM of three separate experiments. Histological sections from fixed ovary tissues of the same mice (center panels) revealed premature meiotic spindle formation in mutants. Extracts from prepubertal PMSG-primed antral follicles had measurable levels of cGMP in controls, but undetectable levels in mutants (far right, bottom). Data are the mean ± SEM of three separate experiments. (**B**) Superovulated prepubertal wild-type (+/+) mice released normal eggs, whereas nearly all mutant oocytes underwent fragmentation. When wild-type and *Npr2*$^{pwe/pwe}$ females were superovulated and mated with wild-type males, *Npr2*$^{pwe/pwe}$ females (black bars) released fewer oocytes compared with the wild-type (white bars). Most of the mutant oocytes were not fertilized and mutant zygotes failed to develop to two-cell embryos. Data are expressed as mean ± SEM (control, $n = 6$; mutant, $n = 4$).

hypothalamic stimulation of the pituitary by pulsatile GnRH secretion and pituitary secretion of FSH and LH (33) are occurring. This is surprising, given that *Npr2* is expressed at all points of the female HPG axis (18,25–28), and natriuretic peptide signaling through NPR2 was proposed to play a role in gonadotropin production (27). Importantly, this work and the work of others (52) clearly demonstrate that *Npr2* signaling is not required for HPG axis function in the female in the context of this genetic background.

The primary cause of female infertility in *Npr2*$^{pwe/pwe}$ females is premature oocyte meiotic resumption. We show that in *Npr2*$^{pwe/pwe}$ mice, impaired cGMP production in ovarian follicles is associated with premature oocyte maturation and impaired embryonic development. Our findings support the requirement for NPR2 to maintain the production of cGMP in ovarian follicles to ensure oocyte meiotic arrest (25). Although *Npr2*$^{pwe/pwe}$ females are able to ovulate in response to exogenous or endogenous gonadotropin stimulation, the oocytes undergo fragmentation (39). This has been reported in *Npr2*$^{cn/cn}$ mutants, mice with reduced levels of CNP (*Nppc*$^{lbab/lbab}$), and in the G-protein coupled receptor 3 mutant mouse (*Gpr3*$^{-/-}$) (52). *Gpr3*$^{-/-}$ oocytes have reduced levels of cAMP, leading to premature meiotic resumption and oocyte fragmentation (39). Taken together, the primary site of *Npr2*$^{pwe/pwe}$ female infertility is the oocyte. None of the descriptions of people affected with AMDM discuss female fertility (16,17,20,53,54). Our studies suggest that if AMDM female patients are infertile due to a failure to maintain oocyte meiotic arrest, they may be able to bear children using donor eggs, provided that uterine and placental function are normal.

Endochondral bone ossification involves the differentiation of condensed mesenchymal cells into chondrocytes that will proliferate and undergo terminal hypertrophic differentiation to ultimately promote the vascularization, mineralization, and recruitment of osteoclasts and osteoblasts into the

Table 2. Normal hormone levels in *peewee* females

Hormone	Unaffected	*peewee*
FSH[a] (ng/ml)	16.9 ± 10.8	17.8 ± 8.6
Estradiol[b] (pg/ml)	16.4 ± 4.7	15.1 ± 3.8

[a]Multiplex testing on serum samples collected at diestrus (control, $n = 8$; *peewee*, $n = 8$).
[b]ELISA on serum samples collected at diestrus (control, $n = 8$; *peewee*, $n = 8$).

nascent element (1,5,6). The trabecular and cortical tissue mineral density of femurs and L4 vertebral elements are normal in *Npr2*$^{pwe/pwe}$ mice, even though the receptor is expressed in osteoblasts (41). It is clear that the main role of the CNP-NPR2 signaling axis in skeletal elements is to regulate their longitudinal growth through action in the growth plate. Without *Npr2,* chondrocyte hypertrophy is compromised, so the bones of mutant animals will never reach a normal adult length, although the bone tissue laid down is normal in its composition.

Both the proliferative and hypertrophic zones of the growth plates in *Npr2*$^{pwe/pwe}$ animals appear reduced in size, consistent with the *Npr2* KO mouse (21) and other spontaneous mutant alleles of *Npr2* (22,23). The loss of *Npr2* does not affect the overall organization of the growth plate, but probably affects either the overall number of chondrocytes recruited to undergo hypertrophic differentiation, the rate in which they commit to this fate, and/or the rate in which they proliferate. We observed elevated activation of ERK1/2 in whole mutant tibial lysates, which demonstrates that NPR2 is required for ERK1/2 inhibition *in vivo*, as predicted by *in vitro* cell culture studies (43).

Treatment for skeletal dysplasia involves multiple lengthening surgeries for the long bones (1,45). These surgeries are expensive, time consuming, fraught with many possible complications, and ultimately result in only a modest increase in bone length (1,45). In general, the acceptance of short stature is advocated in the USA by patients, their families, and advocacy groups for individuals with severe short stature (1). There are currently no effective pharmacological therapies for individuals with skeletal dysplasia (1). Growth hormone treatment has been attempted in achondroplasia patients without much success (1,45). C-type natriuretic peptide (CNP), the ligand of NPR2, is a very promising new therapeutic candidate that has been shown to rescue growth defects in mouse models of achondroplasia both genetically and pharmacologically (7,49,55,56). While this therapeutic approach could offer hope for achondroplasia patients and their families, this form of therapy would be ineffective in AMDM patients that lack the receptor for CNP (16).

There are no reports of growth promoting pharmacotherapy for *Npr2* mutants. Here, we report successful elongation of *Npr2*$^{pwe/pwe}$-mutant tibiae and inhibition of MEK/ERK MAPK signaling within these tibial explants through utilization of the MEK1/2 inhibitors U0126 and PD325901. We also show that MEK1/2 inhibitor treatment extends the length of the hypertrophic zone, consistent with the proposed role of ERK1/2 inhibition in the promotion of hypertrophic differentiation (7,43,49,57). PD325901 treatment led to a more dramatic increase in the tibial length compared with U0126. This could be due to the fact that PD325901 is known to be a more potent MEK1/2 inhibitor, and has been successfully administered to the whole animal in cancer studies (47,58). PD325901 has also been administered orally in clinical trials (59,60). Thus, PD325901 as well as other structurally related agents that are currently undergoing clinical evaluation in cancer are promising therapeutic candidates for growth defects associated with excess MEK1/2 signaling, including patients with AMDM, achondroplasia or other appropriate skeletal dysplasias. The key to moving skeletal dysplasia therapeutics forward will be to deliver this class of agents specifically to the growth plate, and individuals with expertise in the realm of pharmacology will be better suited to address this issue.

We have identified a novel null allele of *Npr2* and characterized the effect on long bone growth and female fertility. In addition, we have established a proof of principle for pharmacotherapy to correct poor bone growth. The next challenge is to develop efficacious delivery methods and treatment regimes in intact animals, minimizing effects on other tissues.

MATERIALS AND METHODS

Generation of *peewee* mice and mapping of the mutation

The *peewee* mutation arose spontaneously on the NAW/WI strain in Glen Wolfe's laboratory at the University of Kansas (Lawrence, KS). The mice were then transferred to Andrzej Bartke's laboratory at Southern Illinois University (SIU, Carbondale, IL). The line was maintained at SIU by outcrossing for hybrid vigor. Upon transfer to the University of Michigan, *in vitro* fertilization was carried out with oocytes from C57BL/6J females (The Jackson Laboratory, Bar Harbor, ME) and sperm from a single homozygous *peewee* male from a mixed background including contributions from the NAW/WI, C57BL/6 and C3H/HeJ strains. The fertilized eggs were transferred to surrogate mothers yielding *pwe* heterozygotes that were a mixture of all these backgrounds. Heterozygotes were bred to (C57BL/6J X C3H/HeJ) F1 mice (The Jackson Laboratory, Bar Harbor, ME), and the heterozygous progeny of this cross were intercrossed to generate mutant animals for analysis. These *pwe* heterozygotes were also crossed to *Mus castaneus* and F1 progeny were intercrossed to map the mutation by genotyping SNPs (19) and microsatellite markers.

All mice were housed in a specific pathogen free facility with 12 h light, 12 h dark cycle in ventilated cages with unlimited access to tap water and Purina 5020 chow. All procedures using mice were approved by the University of Michigan Committee on Use and Care of Animals, and all experiments were conducted in accordance with the principles and procedures outlined in the National Institutes of Health Guidelines of the Care and Use of Experimental Animals.

Skeletal preparation and histology

Skeletal preparations of whole, skinned adult mice were prepared by fixation in 95% ethanol overnight, stained with Alcian Blue, treated with 2% KOH, stained with Alizarin

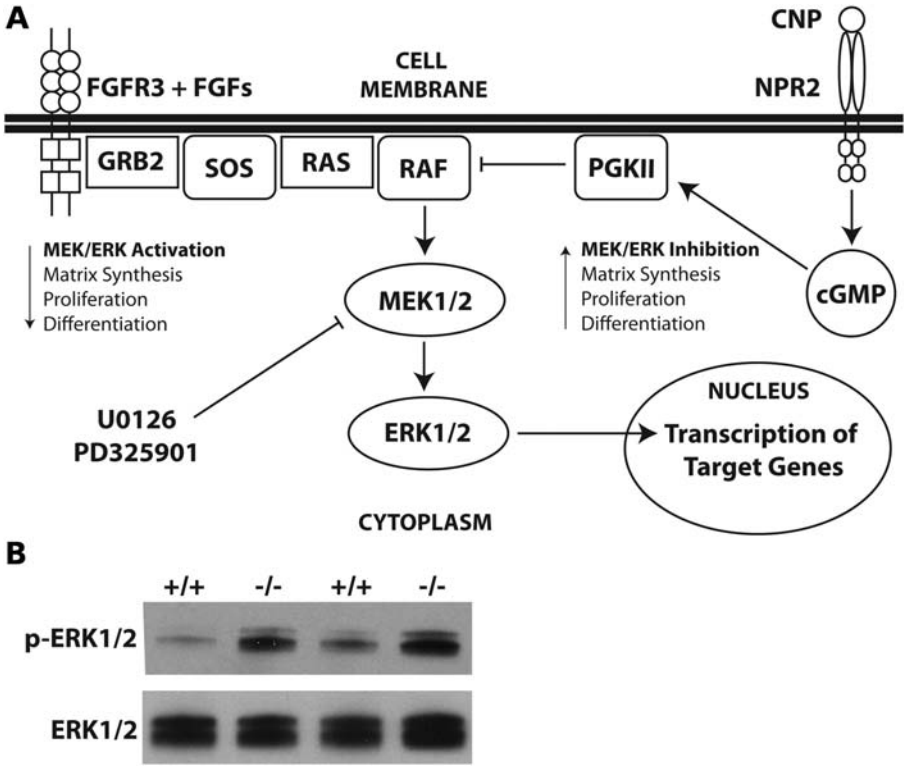

Figure 6. FGF and CNP signaling pathways converge at the MEK/ERK pathway and *Npr2*$^{pwe/pwe}$ mutants have elevated phosphorylated ERK1/2. (**A**) Diagram detailing the key components involved in the FGF and CNP pathways in the growth plate, and the outcomes of activation of these pathways (7,43,44,49,56,66). (**B**) Western blots on postnatal day 3 individual tibial lysates (1 tibia per lane) indicate that *Npr2*$^{pwe/pwe}$ tibiae (−/−) have elevated levels of phosphorylated ERK1/2 (p-ERK1/2) relative to wild-type (+/+) but similar levels of total ERK1/2. Blot images are representative exposures of membranes incubated first with p-ERK1/2 primary antibody, stripped and incubated with total ERK1/2 primary antibody.

Red and stored in glycerol. Bones from affected and unaffected animals were measured with calipers for determination of disproportionate dwarfism. Five-week-old male tibiae were fixed overnight in 4% formaldehyde in phosphate buffered saline (PBS), decalcified as described previously (61), dehydrated through an ethanol series and embedded in paraffin. Tibiae were sectioned and stained with hemotoxylin and eosin.

Analysis of the onset of puberty and estrous cyclicity

Females were observed for date of vaginal opening daily from P18–P28, and estrous cycles were monitored by vaginal cytology every day for a 20-day period between 8 and 12 weeks of age as described (29).

Hormone measurements

Females were sacrificed at 12 weeks of age at diestrus. Serum was prepared from blood samples after clotting for 90 min at room temperature, running a wooden toothpick along the sides of the collection tube and spinning the samples at 2000 *g* for 15 min. The serum supernatant was removed and stored at −20°C until analysis. Analysis was performed by the University of Virginia Ligand Core.

Analysis of oocytes, ovaries and uterus

Prepubertal female mice were stimulated with 5 IU PMSG to stimulate follicle growth to the preovulatory follicle stage and were euthanized 46 h later (62). Oocytes were released from antral follicles from one ovary by needle puncture. The other ovary was fixed overnight in Bouin's fixative (Ricca Chemicals), dehydrated in an ethanol series, followed by *n*-butanol and embedded in paraffin. Sections were stained with Mayer's hemotoxylin and eosin. Uteri were dissected from 12-week-old females at diestrus, fixed for 1 h in 4% paraformaldehyde, dehydrated through an ethanol series and embedded in paraffin. Sections were stained with hemotoxylin and eosin.

cGMP quantification

Intact antral follicles were dissected from PMSG-primed ovaries of mutant and control females as previously described (63). The follicles were processed for cGMP quantification according to the manufacturer's instructions (Cyclic GMP EIA Assay, Cayman Chemical # 581021).

Superovulation

Prepubertal females were stimulated with 5 IU PMSG followed 46 h later by 5 IU human chorionic gonadotropin (hCG) to induce the superovulation of oocytes (62) and placed with an experienced wild-type male overnight. The

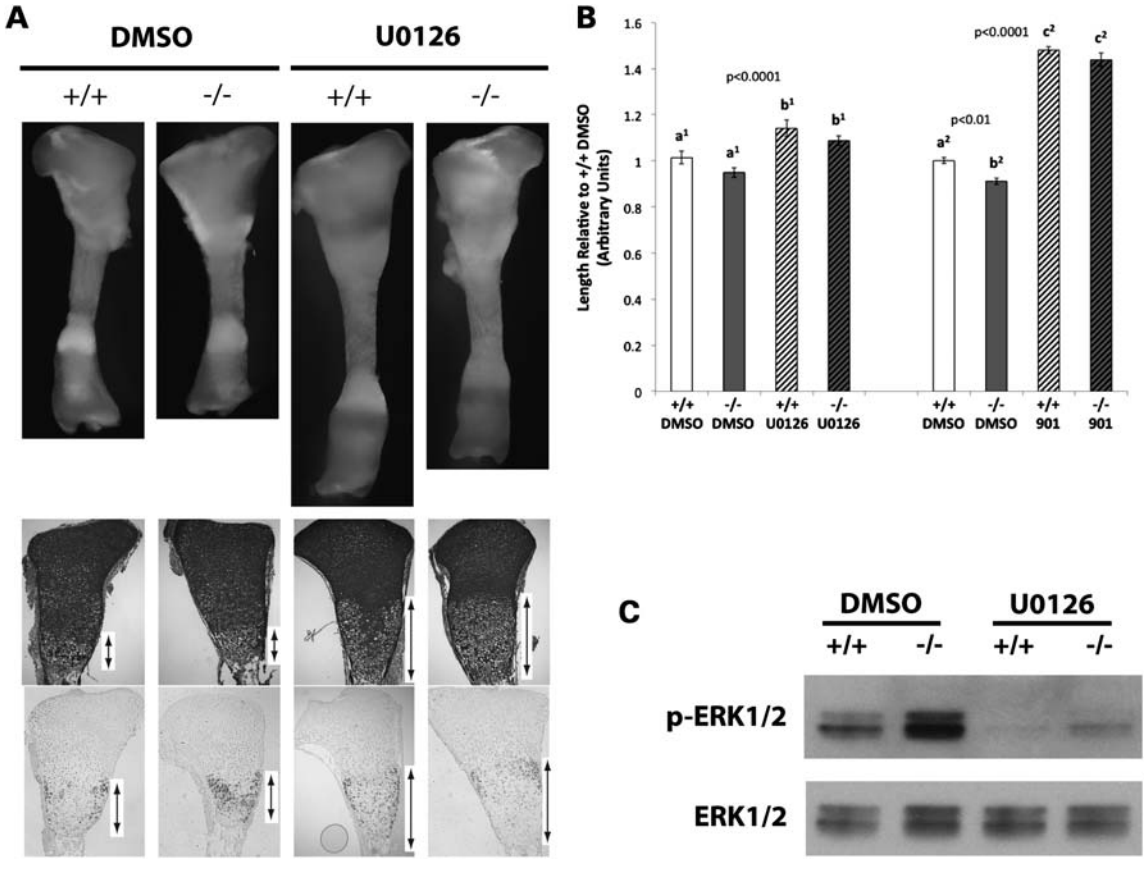

Figure 7. MEK1/2 inhibitors rescue the *Npr2*$^{pwe/pwe}$ growth defect in explants. (**A**) Treatment with the inhibitor U0126 increases the length of mutant and wild-type tibiae by increasing the hypertrophic zone. Both wild-type and mutant whole tibiae are obviously longer than their DMSO (vehicle)-treated contralateral controls. Sections stained with nuclear fast red and alcian blue show the expansion of the hypertrophic zone (vertical arrows) upon treatment. *In situ* hybridization reveals *Col10a1* transcripts in the hypertrophic zone of all samples. (**B**) Quantification of the tibial length in U0126 ($n = 16$ for both genotypes) and PD325901 (901) ($n = 7$ for both genotypes) treated mutants ($-/-$) relative to wild-type ($+/+$). Treatment of both genotypes with either inhibitor leads to a highly significant increase in length ($P < 0.0001$). The PD325901-treated cohort is significantly longer than those treated with U0126 ($P < 0.01$). Letters indicate groups that are significantly different from one another (a,b,c), while the superscript numbers indicate the two different treatment groups (1: U0126, 2: PD325901) (**C**) Western blot analysis of phosphorylated ERK1/2 conducted on U0126-treated tibiae of both genotypes harvested at E16.5 and cultured in the presence of a vehicle (DMSO) or U0126 for 6 days indicates that U0126 inhibits activation of ERK1/2 without altering the levels of total ERK1/2 protein. Each lane contains lysates pooled from four individual tibiae of each genotype and treatment. Blot images are representative exposures of membranes incubated first with p-ERK1/2 primary antibody, stripped and incubated with total ERK1/2 primary antibody.

morning after hCG administration, females were observed for a copulation plug, and fertilized eggs were collected, counted and cultured in M16 media at 37°C in 5% CO_2 for 4 days to observe normal early embryonic development (62).

Natural mating experiments

Twelve-week-old mutant and control females were placed with an experienced hybrid male (C57BL/6J X C3H/HeJ F1, The Jackson Laboratory, Bar Harbor, ME) for a week and observed daily for evidence of a copulation plug. The day of the plug, females were euthanized and their oviducts were flushed with a blunted needle filled with a 6% bovine serum albumin (BSA)/1 × PBS solution. Oocytes were counted under a dissection microscope.

Micro-computed tomography

Specimens were dissected free of soft tissue and analyzed by micro-computed tomography (μCT, eXplore Locus SP, GE Healthcare Pre-Clinical Imaging, London, ON, Canada). Specimens were immersed in water and scanned 4 (femora) or 12 (vertebrae) at a time using the Parker method (180° plus a 20° fan angle) rotated at 80 kVp and 80 μA and filtered using both an acrylic beam flattener and a 0.02 in. aluminum filter. Images were reconstructed at an isotropic voxel size of 18 μm and calibrated for densitometry. A region of interest 20 and 25% of the mid-diaphysis was isolated from the femora for trabecular and cortical analyses, respectively. A region of interest including centrum of the vertebrae and excluding the spinal processes was segmented out for trabecular analysis. Manufacturer software (MicroView v2.2, GE Healthcare Pre-Clinical Imaging) was used to calculate the trabecular bone volume fraction, bone surface-to-volume ratio, thickness (Tb.Th), number (*N*) and spacing (Tb.Sp) along with the bone mineral content, tissue mineral density, and periosteal and endosteal perimeters after applying a uniform threshold of 1200 Hounsfield Units (HU) for trabecular analyses and 2000 HU for cortical analyses.

Tibial cultures and analysis

Tibial cultures were performed as previously described (21). U0126 was purchased from Promega (#V1121), and PD325901 was purchased from LC Laboratories (#P-9688). Both of these inhibitors were used at a final concentration of 10 μM. On the sixth day of culture, tibiae were photographed with a 2.5× objective lens under a dissection microscope and used for histological analysis or frozen at −80°C for protein analysis. Enlarged photographs were printed and measured with a ruler in centimeters to determine their lengths in arbitrary units. For histological analysis, cultured tibiae were fixed overnight in 4% formaldehyde in PBS, dehydrated through an ethanol series and embedded in paraffin. Nuclear Fast Red/Alcian Blue staining was performed as previously described (64). *In situ* hybridizations were performed as previously described (65). The *Col10a1* probe (51) was a generous gift from Ernestina Schipani (Indiana University).

Western blotting

Total protein from cultured tibiae and P3 tibiae was extracted in a T-PER® buffer (Thermo/Pierce #78510) and Halt™ protease and Phosphatase Inhibitor Cocktail (Thermo/Pierce #78440). Total protein was quantified using a BCA protein assay kit (Thermo/Pierce #23225). Proteins and ladder (BIO-RAD #161-0375) were run on 4–20% Mini-Protean® TGX™ Gels from BIO-RAD (#456-1093S (10 well)) and transferred to an Amersham Hybond™-P membrane (GE Healthcare). Membranes were washed with a standard Tris-buffered saline solution using Tween-20 (TBS-Tween). ERK antibodies were purchased from Cell Signaling Technology (phospho-ERK1/2: #4370, total ERK1/2: #4695) and diluted as per the manufacturer's instructions. Anti-beta actin was obtained from Abcam and used at a 1:2500 dilution. Goat-anti-rabbit conjugated to horseradish peroxidase secondary antibody was purchased from Thermo Scientific (#31462) and was diluted to 1:25 000. Membranes were blocked and incubated with an antibody in a 1% BSA/TBS-Tween solution. BSA was purchased from Cell Signaling Technology (#9998S). Membranes were developed with the SuperSignal® West Pico chemiluminescent substrate (Thermo/Pierce #34080) and stripped with Restore™ western blot stripping buffer (Thermo/Pierce #21059).

AUTHORS' CONTRIBUTIONS

K.A.G.: intellectual force in identification of the mutation, concept and execution of pharmacotherapy; histology of the skeleton, uterus and ovary; puberty and estrus assessments; wrote the manuscript with editing by S.A.C. M.L.B.: sequenced several candidate genes. M.H. and M.C.: meiotic arrest. S.M.F.: male fertility assessment. I.J.K.: skeletal preparations and measurements, intersubspecific cross for genetic mapping. J.E.P. and K.M.K.: MicroCT analysis.

SUPPLEMENTARY MATERIAL

Supplementary Material is available at *HMG* online.

ACKNOWLEDGEMENTS

We thank the University of Michigan Sequencing Core and Transgenic Animal Model Core Facilities, especially Bob Lyons, Galina Gavrilina, the late Maggie Van Keuren and Thomas L. Saunders. We thank Andrzej Bartke, Glen Wolfe, Daniel Turyn (U. Buenos Aires), Jackie Collins, Terry Parkening, Kurt Borg and Artur Mayerhofer for early analysis of the spontaneous mutant. We thank Jeffrey Innis, Thomas Peedikayil, Judith Leopold, Miriam Meisler and Autumn Wenglikowski for their contributions. We acknowledge David Beier and Jennifer Moran for performing the initial genome-wide SNP mapping of the *Npr2*$^{pwe/pwe}$ mutation.

Conflict of Interest statement. None declared.

FUNDING

This work is supported by the University of Michigan James V. Neel Professorship Funds (S.A.C.), Regents' Fellowship for Cellular and Molecular Biology and Rackham Graduate School, (K.A.G.).

REFERENCES

1. Krakow, D. and Rimoin, D.L. (2010) The skeletal dysplasias. *Genet. Med.*, **12**, 327–341.
2. Dighe, M., Fligner, C., Cheng, E., Warren, B. and Dubinsky, T. (2008) Fetal skeletal dysplasia: an approach to diagnosis with illustrative cases. *Radiographics*, **28**, 1061–1077.
3. Superti-Furga, A. and Unger, S. (2007) Nosology and classification of genetic skeletal disorders: 2006 revision. *Am. J. Med. Genet. A*, **143**, 1–18.
4. Warman, M.L., Cormier-Daire, V., Hall, C., Krakow, D., Lachman, R., LeMerrer, M., Mortier, G., Mundlos, S., Nishimura, G., Rimoin, D.L. *et al.* (2011) Nosology and classification of genetic skeletal disorders: 2010 revision. *Am. J. Med. Genet. A*, **155A**, 943–968.
5. Mackie, E.J., Tatarczuch, L. and Mirams, M. (2011) The skeleton: a multi-functional complex organ: the growth plate chondrocyte and endochondral ossification. *J. Endocrinol.*, **211**, 109–121.
6. Karsenty, G., Kronenberg, H.M. and Settembre, C. (2009) Genetic control of bone formation. *Annu. Rev. Cell. Dev. Biol.*, **25**, 629–648.
7. Baldridge, D., Shchelochkov, O., Kelley, B. and Lee, B. (2010) Signaling pathways in human skeletal dysplasias. *Annu. Rev. Genomics Hum. Genet.*, **11**, 189–217.
8. Lee, H., Graham, J.M. Jr, Rimoin, D.L., Lachman, R.S., Krejci, P., Tompson, S.W., Nelson, S.F., Krakow, D. and Cohn, D.H. (2012) Exome sequencing identifies PDE4D mutations in acrodysostosis. *Am. J. Hum. Genet.*, **90**, 746–751.
9. Sybert, V.P. and McCauley, E. (2004) Turner's syndrome. *N. Engl. J. Med.*, **351**, 1227–1238.
10. Velagaleti, G.V., Bien-Willner, G.A., Northup, J.K., Lockhart, L.H., Hawkins, J.C., Jalal, S.M., Withers, M., Lupski, J.R. and Stankiewicz, P. (2005) Position effects due to chromosome breakpoints that map approximately 900 kb upstream and approximately 1.3 Mb downstream of SOX9 in two patients with campomelic dysplasia. *Am. J. Hum. Genet.*, **76**, 652–662.
11. Arboleda, V.A., Lee, H., Parnaik, R., Fleming, A., Banerjee, A., Ferraz-de-Souza, B., Delot, E.C., Rodriguez-Fernandez, I.A., Braslavsky, D., Bergada, I. *et al.* (2012) Mutations in the PCNA-binding domain of CDKN1C cause IMAGe syndrome. *Nat. Genet.*, **44**, 788–792.
12. Matzuk, M.M. and Lamb, D.J. (2002) Genetic dissection of mammalian fertility pathways. *Nat. Cell. Biol.*, **4**(suppl.), s41–s49.
13. Tatone, C., Amicarelli, F., Carbone, M.C., Monteleone, P., Caserta, D., Marci, R., Artini, P.G., Piomboni, P. and Focarelli, R. (2008) Cellular and molecular aspects of ovarian follicle ageing. *Hum. Reprod. Update*, **14**, 131–142.

14. Matzuk, M.M. and Lamb, D.J. (2008) The biology of infertility: research advances and clinical challenges. *Nat. Med.*, **14**, 1197–1213.
15. Barnett, K.R., Schilling, C., Greenfeld, C.R., Tomic, D. and Flaws, J.A. (2006) Ovarian follicle development and transgenic mouse models. *Hum. Reprod. Update*, **12**, 537–555.
16. Bartels, C.F., Bukulmez, H., Padayatti, P., Rhee, D.K., van Ravenswaaij-Arts, C., Pauli, R.M., Mundlos, S., Chitayat, D., Shih, L.Y., Al-Gazali, L.I. *et al.* (2004) Mutations in the transmembrane natriuretic peptide receptor NPR-B impair skeletal growth and cause acromesomelic dysplasia, type Maroteaux. *Am. J. Hum. Genet.*, **75**, 27–34.
17. Kant, S.G., Polinkovsky, A., Mundlos, S., Zabel, B., Thomeer, R.T., Zonderland, H.M., Shih, L., van Haeringen, A. and Warman, M.L. (1998) Acromesomelic dysplasia Maroteaux type maps to human chromosome 9. *Am. J. Hum. Genet.*, **63**, 155–162.
18. Potter, L.R. (2011) Guanylyl cyclase structure, function and regulation. *Cell. Signal.*, **23**, 1921–1926.
19. Moran, J.L., Bolton, A.D., Tran, P.V., Brown, A., Dwyer, N.D., Manning, D.K., Bjork, B.C., Li, C., Montgomery, K., Siepka, S.M. *et al.* (2006) Utilization of a whole genome SNP panel for efficient genetic mapping in the mouse. *Genome Res.*, **16**, 436–440.
20. Hachiya, R., Ohashi, Y., Kamei, Y., Suganami, T., Mochizuki, H., Mitsui, N., Saitoh, M., Sakuragi, M., Nishimura, G., Ohashi, H. *et al.* (2007) Intact kinase homology domain of natriuretic peptide receptor-B is essential for skeletal development. *J. Clin. Endocrinol. Metab.*, **92**, 4009–4014.
21. Tamura, N., Doolittle, L.K., Hammer, R.E., Shelton, J.M., Richardson, J.A. and Garbers, D.L. (2004) Critical roles of the guanylyl cyclase B receptor in endochondral ossification and development of female reproductive organs. *Proc. Natl Acad. Sci. USA*, **101**, 17300–17305.
22. Tsuji, T. and Kunieda, T. (2005) A loss-of-function mutation in natriuretic peptide receptor 2 (Npr2) gene is responsible for disproportionate dwarfism in cn/cn mouse. *J. Biol. Chem.*, **280**, 14288–14292.
23. Sogawa, C., Tsuji, T., Shinkai, Y., Katayama, K. and Kunieda, T. (2007) Short-limbed dwarfism: slw is a new allele of Npr2 causing chondrodysplasia. *J. Hered.*, **98**, 575–580.
24. Sogawa, C., Abe, A., Tsuji, T., Koizumi, M., Saga, T. and Kunieda, T. (2010) Gastrointestinal tract disorder in natriuretic peptide receptor B gene mutant mice. *Am. J. Pathol.*, **177**, 822–828.
25. Zhang, M., Su, Y.Q., Sugiura, K., Xia, G. and Eppig, J.J. (2010) Granulosa cell ligand NPPC and its receptor NPR2 maintain meiotic arrest in mouse oocytes. *Science*, **330**, 366–369.
26. Fowkes, R.C. and McArdle, C.A. (2000) C-type natriuretic peptide: an important neuroendocrine regulator? Trends Endocrinol. Metab., **11**, 333–338.
27. Thompson, I.R., Chand, A.N., Jonas, K.C., Burrin, J.M., Steinhelper, M.E., Wheeler-Jones, C.P., McArdle, C.A. and Fowkes, R.C. (2009) Molecular characterisation and functional interrogation of a local natriuretic peptide system in rodent pituitaries, alphaT3-1 and LbetaT2 gonadotroph cells. *J. Endocrinol.*, **203**, 215–229.
28. Dos Reis, A.M., Fujio, N., Dam, T.V., Mukaddam-Daher, S., Jankowski, M., Tremblay, J. and Gutkowska, J. (1995) Characterization and distribution of natriuretic peptide receptors in the rat uterus. *Endocrinology*, **136**, 4247–4253.
29. Caligioni, C.S. (2009) Assessing reproductive status/stages in mice. *Curr. Protoc. Neurosci.*, Appendix 4, Appendix 4I, Supplement 48.
30. Daftary, S.S. and Gore, A.C. (2005) IGF-1 in the brain as a regulator of reproductive neuroendocrine function. *Exp. Biol. Med. (Maywood)*, **230**, 292–306.
31. Chandrashekar, V., Zaczek, D. and Bartke, A. (2004) The consequences of altered somatotropic system on reproduction. *Biol. Reprod.*, **71**, 17–27.
32. DiVall, S.A. and Radovick, S. (2008) Pubertal development and menarche. *Ann. NY Acad. Sci.*, **1135**, 19–28.
33. Cone, R.D., Low, M.J., Elmquist, J.K. and Cameron, J.L. (2003) In Larsen, P.R., Kronenberg, H.M., Melmed, S. and Polonsky, K.S. (eds), *Williams Textbook of Endocrinology*. Saunders, Philadelphia, pp. 81–176.
34. Zhang, M., Ouyang, H. and Xia, G. (2009) The signal pathway of gonadotrophins-induced mammalian oocyte meiotic resumption. *Mol. Hum. Reprod.*, **15**, 399–409.
35. Mehlmann, L.M. (2005) Stops and starts in mammalian oocytes: recent advances in understanding the regulation of meiotic arrest and oocyte maturation. *Reproduction*, **130**, 791–799.
36. Sun, Q.Y., Miao, Y.L. and Schatten, H. (2009) Towards a new understanding on the regulation of mammalian oocyte meiosis resumption. *Cell Cycle*, **8**, 2741–2747.
37. Vaccari, S., Weeks, J.L. II, Hsieh, M., Menniti, F.S. and Conti, M. (2009) Cyclic GMP signaling is involved in the luteinizing hormone-dependent meiotic maturation of mouse oocytes. *Biol. Reprod.*, **81**, 595–604.
38. Norris, R.P., Ratzan, W.J., Freudzon, M., Mehlmann, L.M., Krall, J., Movsesian, M.A., Wang, H., Ke, H., Nikolaev, V.O. and Jaffe, L.A. (2009) Cyclic GMP from the surrounding somatic cells regulates cyclic AMP and meiosis in the mouse oocyte. *Development*, **136**, 1869–1878.
39. Ledent, C., Demeestere, I., Blum, D., Petermans, J., Hamalainen, T., Smits, G. and Vassart, G. (2005) Premature ovarian aging in mice deficient for Gpr3. *Proc. Natl Acad. Sci. USA*, **102**, 8922–8926.
40. Bulun, S.E. and Adashi, E.Y. (2003) In Larsen, P.R., Kronenberg, H.M., Melmed, S. and Polonsky, K.S. (eds), *Williams Textbook of Endocrinology*. Saunders, Philadelphia, pp. 587–664.
41. Kaneki, H., Kurokawa, M. and Ide, H. (2008) The receptor attributable to C-type natriuretic peptide-induced differentiation of osteoblasts is switched from type B- to type C-natriuretic peptide receptor with aging. *J. Cell. Biochem.*, **103**, 753–764.
42. Yeh, L.C., Zavala, M.C. and Lee, J.C. (2006) C-type natriuretic peptide enhances osteogenic protein-1-induced osteoblastic cell differentiation via Smad5 phosphorylation. *J. Cell Biochem.*, **97**, 494–500.
43. Krejci, P., Masri, B., Fontaine, V., Mekikian, P.B., Weis, M., Prats, H. and Wilcox, W.R. (2005) Interaction of fibroblast growth factor and C-natriuretic peptide signaling in regulation of chondrocyte proliferation and extracellular matrix homeostasis. *J. Cell Sci.*, **118**, 5089–5100.
44. Horton, W.A. and Degnin, C.R. (2009) FGFs in endochondral skeletal development. *Trends Endocrinol. Metab.*, **20**, 341–348.
45. Shirley, E.D. and Ain, M.C. (2009) Achondroplasia: manifestations and treatment. *J. Am. Acad. Orthop. Surg.*, **17**, 231–241.
46. Lauchle, J.O., Kim, D., Le, D.T., Akagi, K., Crone, M., Krisman, K., Warner, K., Bonifas, J.M., Li, Q., Coakley, K.M. *et al.* (2009) Response and resistance to MEK inhibition in leukaemias initiated by hyperactive Ras. *Nature*, **461**, 411–414.
47. Lyubynska, N., Gorman, M.F., Lauchle, J.O., Hong, W.X., Akutagawa, J.K., Shannon, K. and Braun, B.S. (2011) A MEK inhibitor abrogates myeloproliferative disease in Kras mutant mice. *Sci. Transl. Med.*, **3**, 76ra27.
48. Shukla, V., Coumoul, X., Wang, R.H., Kim, H.S. and Deng, C.X. (2007) RNA interference and inhibition of MEK-ERK signaling prevent abnormal skeletal phenotypes in a mouse model of craniosynostosis. *Nat. Genet.*, **39**, 1145–1150.
49. Yasoda, A., Komatsu, Y., Chusho, H., Miyazawa, T., Ozasa, A., Miura, M., Kurihara, T., Rogi, T., Tanaka, S., Suda, M. *et al.* (2004) Overexpression of CNP in chondrocytes rescues achondroplasia through a MAPK-dependent pathway. *Nat. Med.*, **10**, 80–86.
50. Barrett, S.D., Bridges, A.J., Dudley, D.T., Saltiel, A.R., Fergus, J.H., Flamme, C.M., Delaney, A.M., Kaufman, M., LePage, S., Leopold, W.R. *et al.* (2008) The discovery of the benzhydroxamate MEK inhibitors CI-1040 and PD 0325901. *Bioorg. Med. Chem. Lett.*, **18**, 6501–6504.
51. Araldi, E., Khatri, R., Giaccia, A.J., Simon, M.C. and Schipani, E. (2011) Lack of HIF-2alpha in limb bud mesenchyme causes a modest and transient delay of endochondral bone development. *Nat. Med.*, **17**, 25–26; author reply 27–29.
52. Kiyosu, C., Tsuji, T., Yamada, K., Kajita, S. and Kunieda, T. (2012) NPPC/NPR2 signaling is essential for oocyte meiotic arrest and cumulus oophorus formation during follicular development in the mouse ovary. *Reproduction*., **144**, 187–193.
53. Khan, S., Hussain Ali, R., Abbasi, S., Nawaz, M., Muhammad, N. and Ahmad, W. (2012) Novel mutations in natriuretic peptide receptor-2 gene underlie acromesomelic dysplasia, type maroteaux. *BMC Med. Genet.*, **13**, 44.
54. Olney, R.C., Bukulmez, H., Bartels, C.F., Prickett, T.C., Espiner, E.A., Potter, L.R. and Warman, M.L. (2006) Heterozygous mutations in natriuretic peptide receptor-B (NPR2) are associated with short stature. *J. Clin. Endocrinol. Metab.*, **91**, 1229–1232.
55. Yasoda, A., Kitamura, H., Fujii, T., Kondo, E., Murao, N., Miura, M., Kanamoto, N., Komatsu, Y., Arai, H. and Nakao, K. (2009) Systemic administration of C-type natriuretic peptide as a novel therapeutic strategy for skeletal dysplasias. *Endocrinology*, **150**, 3138–3144.
56. Yasoda, A. and Nakao, K. (2010) Translational research of C-type natriuretic peptide (CNP) into skeletal dysplasias. *Endocr. J.*, **57**, 659–666.

57. Foldynova-Trantirkova, S., Wilcox, W.R. and Krejci, P. (2012) Sixteen years and counting: the current understanding of fibroblast growth factor receptor 3 (FGFR3) signaling in skeletal dysplasias. *Hum. Mutat.*, **33**, 29–41.
58. Solit, D.B., Garraway, L.A., Pratilas, C.A., Sawai, A., Getz, G., Basso, A., Ye, Q., Lobo, J.M., She, Y., Osman, I. *et al.* (2006) BRAF mutation predicts sensitivity to MEK inhibition. *Nature*, **439**, 358–362.
59. Boasberg, P.D., Redfern, C.H., Daniels, G.A., Bodkin, D., Garrett, C.R. and Ricart, A.D. (2011) Pilot study of PD-0325901 in previously treated patients with advanced melanoma, breast cancer, and colon cancer. *Cancer Chemother. Pharmacol.*, **68**, 547–552.
60. Haura, E.B., Ricart, A.D., Larson, T.G., Stella, P.J., Bazhenova, L., Miller, V.A., Cohen, R.B., Eisenberg, P.D., Selaru, P., Wilner, K.D. *et al.* (2010) A phase II study of PD-0325901, an oral MEK inhibitor, in previously treated patients with advanced non-small cell lung cancer. *Clin. Cancer. Res.*, **16**, 2450–2457.
61. Song, B., Haycraft, C.J., Seo, H.S., Yoder, B.K. and Serra, R. (2007) Development of the post-natal growth plate requires intraflagellar transport proteins. *Dev. Biol.*, **305**, 202–216.
62. Nagy, A., Gertsenstein, M., Vinterstein, K. and Behringer, R. (2003) *Manipulating the Mouse Embryo: A Laboratory Manual*. Cold Spring Harbor Laboratory Press, ColdSpring Harbor.
63. Panigone, S., Hsieh, M., Fu, M., Persani, L. and Conti, M. (2008) Luteinizing hormone signaling in preovulatory follicles involves early activation of the epidermal growth factor receptor pathway. *Mol. Endocrinol.*, **22**, 924–936.
64. Retting, K.N., Song, B., Yoon, B.S. and Lyons, K.M. (2009) BMP canonical Smad signaling through Smad1 and Smad5 is required for endochondral bone formation. *Development*, **136**, 1093–1104.
65. Cushman, L.J., Watkins-Chow, D.E., Brinkmeier, M.L., Raetzman, L.T., Radak, A.L., Lloyd, R.V. and Camper, S.A. (2001) Persistent Prop1 expression delays gonadotrope differentiation and enhances pituitary tumor susceptibility. *Hum. Mol. Genet.*, **10**, 1141–1153.
66. Agoston, H., Khan, S., James, C.G., Gillespie, J.R., Serra, R., Stanton, L.A. and Beier, F. (2007) C-type natriuretic peptide regulates endochondral bone growth through p38 MAP kinase-dependent and -independent pathways. *BMC Dev. Biol.*, **7**, 18.